Available online at www.sciencedirect.com
ScienceDirect
International Journal of Pharmaceutics 355 (2008) 114–125
INTERNATIONAL JOURNAL OF PHARMACEUTICS
www.elsevier.com/locate/ijpharm

Development of a reaction-limited model of dissolution: Application to official dissolution tests experiments

A. Dokoumetzidis [a], V. Papadopoulou [b], G. Valsami [b], P. Macheras [b,*]

[a] *School of Pharmacy and Pharmaceutical Sciences, University of Manchester, Manchester M13 9PT, UK*
[b] *Laboratory of Biopharmaceutics and Pharmacokinetics, Faculty of Pharmacy, University of Athens, Athens 15771, Greece*

Received 15 October 2007; received in revised form 26 November 2007; accepted 29 November 2007
Available online 5 December 2007

Abstract

A reaction-limited model for drug dissolution is developed assuming that the reaction at the solid–liquid interface is controlling the rate of dissolution. The dissolution process is considered as a bidirectional chemical reaction of the undissolved drug species with the free solvent molecules, yielding the dissolved species of drug complex with solvent. This reaction was considered in either sink conditions, where it corresponds to the unidirectional case and the entire amount of the drug is dissolved, or reaching chemical equilibrium, which corresponds to saturation of the solution. The model equation was fitted successfully to dissolution data sets of naproxen and nitrofurantoin formulations measured in the paddle and basket apparatuses, respectively, under various experimental conditions. For comparative purposes these data were also analyzed using three functions based on the diffusion layer model. All functions failed to reveal the governing role of saturation solubility in the dissolution process associated with the diffusion layer model when the conditions for the valid estimation of saturation solubility, established theoretically in this study, were met by the experimental set up employed. Overall, the model developed provides an interesting alternative to the classic approaches of drug dissolution modeling, quantifying the case of reaction-limited dissolution of drugs.

Keywords: Dissolution; Reaction-limited model; Solubility; Dissolution tests

1. Introduction

The history of dissolution starts when Noyes and Whitney (1897) carried out the first dissolution experiments and found that the dissolution rate, (dC/dt), is a linear function of the concentration gradient:

$$\frac{dC_b}{dt} = k_d(C_s - C_b) \quad (1)$$

where k_d is the dissolution rate constant, C_s is the saturation solubility and C_b is the bulk concentration at time t. Later on, Nernst (1904) and Brunner (1904) showed that k_d is a composite constant being proportional to the diffusion coefficient D_C and the surface area of the dissolving body, S. Thus, Eq. (1) was written

$$\frac{dC_b}{dt} = \frac{D_C S}{V \times \delta}(C_s - C_b) \quad (2)$$

where δ designates the width of the region through which the dissolved species diffuse and V is the volume of the dissolution medium.

Dissolution is a classical heterogeneous process since it takes place on the solid–liquid phase boundaries (Levich, 1962). All heterogeneous processes involve several steps. In fact, the dissolution of a solid in an aqueous solution is considered to take place in two steps: (i) a reaction at the solid–liquid interface, the so called "interfacial transport" and (ii) transfer of the dissolved matter away from the reaction site (Dokoumetzidis and Macheras, 2006; Macheras and Iliadis, 2006). The slower of these steps exercises a dominating influence upon the rate of dissolution. In this connection it may be remarked that Eqs. (1) and (2) are used to describe dissolution when the rate of diffusion of the species through the layer surrounding the drug particle is slower than the reaction at the solid–liquid interface. According

* Corresponding author. Tel.: +30 210 7274026; fax: +30 210 7274027.
E-mail address: macheras@pharm.uoa.gr (P. Macheras).

0378-5173/$ – see front matter © 2007 Elsevier B.V. All rights reserved.
doi:10.1016/j.ijpharm.2007.11.056

to Levich (1962), Eq. (2) signifies that the liquid immediately adjacent to the dissolving solid is always saturated. Also, Eq. (2) represents a theoretically sound expression for diffusional flow in a static medium, but it should be regarded as purely empirical when applied to a medium in motion. These observations prompted Levich (1962) to develop in his seminal book the theory of the so called convective diffusion of a solute in liquids and derive an explicit relationship between the thickness (δ) and the agitation rate for the rotating disk device. This theory and all of its advances has been applied to dissolution experiments in rotating or stationary disk apparatuses or flow through cells (Khoury et al., 1988; Missel et al., 2004a,b) under well defined hydrodynamic conditions. One of the key assumptions in all studies is that the solute concentration at the dissolving surface is equal to the solubility limit irrespective of applied hydrodynamic conditions. Moreover, the flux or the dissolution rate is always considered directly proportional to the solubility of the dissolving substance under sink conditions.

Several experimental studies (Touitou and Donbrow, 1981; Kimura et al., 1994; Lin et al., 1995; Sunagawa et al., 1995) have questioned the equilibrium existing at the solid–liquid interface. However, the elegant theoretical analysis of Dejmek and Ward (1998) on crystal growth-dissolution phenomena, based on the statistical rate theory, provides a well founded link between the interfacial transport and the diffusion of species through the diffusion layer. The work of Dejmek and Ward (1998) reveals not only the concurrent contribution of the two mechanisms to the overall dissolution but also the dominating role of the concentration at the liquid/solid interface for the dissolution rate. The results of this study based on a rotating disk apparatus prompted Ji et al. (2001) to propose that the concentration at the interface C_i and not the saturation solubility C_s, controls the rate of dissolution; this hypothesis was expressed mathematically as follows:

$$\frac{dC_b}{dt} = k_d(C_i - C_b) \tag{3}$$

Despite all these advances and the attempts to replace the assumption for the fixed concentration at the solid surface (Missel et al., 2004a) in the dissolution studies, the boundary conditions utilized in the theoretical analysis of dissolution assume that the concentration of the dissolving species at the surface is equal to the solubility limit (Levich, 1962). Besides, the predominant role of saturation solubility in governing the dissolution rate either *in vitro* or *in vivo* is a kind of a dogma in pharmaceutics and biopharmaceutics. In parallel, no attention is paid to a dissolution mechanism based on interfacial transport, the so called reaction-limited model, since a well founded mathematical model has not been proposed so far. Only in early review articles (Wagner, 1961; Higuchi, 1967; Swarbrick, 1970) the rate of drug dissolution, G, that is controlled by the interfacial reaction was reluctantly (Wagner, 1961) expressed as

$$G = k(C_s - C_b) \tag{4}$$

where k is characterized as the "effective interfacial rate constant". Eq. (4) is obviously wrong since (i) the concentration profile of the reactant species near the interface for reaction-limited kinetics is flat and (ii) the concentration gradient in Eq. (4) adheres to the diffusion layer model. The debate on the primary process controlling the dissolution kinetics as a function of agitation conditions has also been presented in the early times of drug dissolution (Wurster and Taylor, 1965). However, more than 30 years ago the seminal work of Tao et al. (1974) on gallstone dissolution demonstrated the importance of interfacial kinetics as well as the effect of the agitation rate on the process controlling the dissolution kinetics. In the same vein, several other groups (Nedich and Kildsig, 1972; Nicklasson et al., 1981, 1983) tried to quantify the process next to the disk surface in the rotating disk i.e. the rate of mass transfer from solid to aqueous phase. In recent years, two approaches, (Dokoumetzidis and Macheras, 1997; Lansky and Weiss, 1999) which were proposed to describe the heterogeneous features of drug dissolution, can be considered as reaction-limited dissolution models since both do not rely on the premises of the diffusion principles.

In parallel, the chemical reaction between a solid and a fluid is the main subject of research in many areas of chemical engineering such as combustion of fuels, reduction of metallic oxides, corrosion of metals, partial dissolution of alloys, heterogeneous catalysis, deactivation of industrial gases by flowing through porous media, petroleum industry, etc. (Daccord, 1989). Extensive applications of dissolution models based on either diffusion- or reaction-limited kinetics can be found in chemical engineering literature (Daccord, 1989; Miller-Chou and Koenig, 2003; Greenberg and Tomson, 1992; Yang and Cussler, 2001; Robertson and Fogler, 1996).

Although the diffusion layer model of dissolution has been exclusively based on experiments in rotating disk or flow through cells under well defined hydrodynamic conditions, diffusional principles are routinely applied in all drug dissolution experiments carried out in official apparatuses. These dissolution experiments in conjunction with the dominating role of saturation solubility in diffusion-limited dissolution kinetics (Eqs. (1) and (2)) are essential elements of the FDA (2000) guidance on the biopharmaceutics classification system. In this study, we question the relative importance of the rate of drug transport across the interface and the diffusion rate in the official dissolution systems. To this end, a novel reaction-limited model of dissolution was developed and applied to a number of naproxen and nitrofurantoin dissolution experiments carried out in the official dissolution systems under various experimental conditions. For comparative purposes the same data were analyzed using three functions based on the diffusion layer model.

2. Theory

2.1. Diffusion limited dissolution models

When one deals with the dissolution of tablets, the drug dose should be taken into account since if this is ignored, Eqs. (1) and (2) incorrectly predict that the saturation solubility will be reached at infinite time regardless the amount (dose, D) of drug used in the experiments. In this regard, Eq. (1) has

been expressed in terms of the fraction of dose dissolved, Φ (Dokoumetzidis et al., 2006):

$$\frac{d\Phi}{dt} = k_d\left(\frac{1}{q} - \Phi\right) \tag{5}$$

where $\Phi = [C] \times V/D$ and $1/q$ is the dimensionless solubility/dose ratio since the volume V of the dissolution medium has been taken into account i.e.

$$q = \frac{D}{C_s V} \tag{6}$$

Integration of Eq. (5) leads to the branched version of the classical exponential form of Noyes–Whitney equation (Dokoumetzidis et al., 2006):

$$\Phi = \begin{cases} \frac{1}{q}(1 - e^{-k_d t}) & \text{for} \quad t < T \quad (\Phi < 1) \\ 1 & \text{for} \quad t \geq T \end{cases} \tag{7}$$

This equation reveals that the value of the fraction of dose dissolved Φ increases exponentially with time and becomes equal to unity only when the entire dose can be dissolved in the dissolution medium. Otherwise, Φ reaches exponentially the steady-state value, $1/q$. The special case of Φ reaching unity in infinite time comes only when $q = 1$.

Eq. (2) does not take into account the changes in the surface of the solid as it dissolves. Writing the surface as a function of the dissolved quantity scaled by the volume ($D/V - C_b$) assuming spherical particle geometry, Eq. (2) can be written as:

$$\frac{dC_b}{dt} = k_s\left(\frac{D}{V} - C_b\right)^{2/3}(C_s - C_b) \tag{8}$$

where k_s is a constant; rewriting Eq. (8) in terms of Φ we end up with:

$$\frac{d\Phi}{dt} = k_s\left(\frac{D}{V}\right)^{2/3}(1 - \Phi)^{2/3}\left(\frac{1}{q} - \Phi\right) \tag{9}$$

Note that Eq. (9) considers that the entire amount may be dissolved only in infinite time and therefore does not need to be branched. Eq. (9) does not have an analytical solution and needs to be solved numerically.

Relying again on the fundamental Eq. (1) and assuming that a time dependent coefficient $k_d = k_D t^{-h}$, and not a dissolution rate constant, governs the dissolution rate (Macheras and Dokoumetzidis, 2000), a branched version of the Weibull function, which is used extensively and successfully in dissolution studies can also be derived (Dokoumetzidis et al., 2006):

$$\Phi = \begin{cases} \frac{1}{q}(1 - e^{-\gamma \times t^{\beta}}) & \text{for} \quad t < T \quad (\Phi < 1) \\ 1 \quad \text{for} \quad t \geq T \end{cases} \tag{10}$$

where γ, β are the scale and shape parameters related to k_d and the dimensionless exponent h, i.e. $\gamma = k_d/(1 - h)$ and $\beta = 1 - h$. The asymptotic values for Φ in Eq. (10) are the same with these described for Eq. (7).

The derivation of Eqs. (7), (9) and (10) relies on the fundamental Eqs. (1) and (2). The governing role of the saturation solubility, C_s in Eqs. (7), (9) and (10) can be easily concluded since C_s is related proportionally with $1/q$ (Eq. (6)). However, if the postulate for the governing role of interfacial concentration, C_i, in the rate of drug dissolution is true, then using Eq. (3) one can derive the equations in an identical manner to that used for the derivation of Eqs. (7), (9) and (10) and the only difference would be that instead of q, it would have q_i.

Estimates for q or q_i can be derived from the fitting of Eqs. (7), (9) and (10) to experimental dissolution data. From this estimate, one can distinguish whether C_s or C_i governs the dissolution rate by comparing it with the value of q derived from Eq. (6) using independent experimental solubility values. Parameters q or q_i cannot be directly determined from the plateau when the entire drug dose is dissolved and their estimation relies on the fitting of Eqs. (7), (9) and (10) to experimental data. However, as described in Appendix A, it is feasible to estimate these parameters with a specific confidence, assuming that the model used is correct.

2.2. A reaction-limited model for dissolution

We assume that the drug particles are dispersed in the dissolution medium. Classical chemical kinetic principles similar to these used in (Lansky and Weiss, 1999) are applied for the description of the dissolution process, which is considered as a bidirectional chemical reaction of the undissolved drug species, s, with n free solvent molecules, w, yielding the dissolved species of drug complex with solvent, c:

$$s + nw \underset{k_{-1}}{\overset{k_1}{\rightleftarrows}} c \tag{11}$$

The above reaction can be considered in either sink conditions, where it corresponds to the unidirectional case and the entire amount of s is dissolved, or reaching chemical equilibrium, which corresponds to saturation of the solution.

The rate of the dissolution process is given by the velocity of the reaction:

$$\frac{d[c]}{dt} = k_1[s]^a \times [w]^b - k_{-1}[c] \tag{12}$$

where $[s]$, $[w]$ and $[c]$ are concentrations in moles per unit volume. Also, a and b are exponents that determine the order of the reaction. These exponents may depend on stoichiometry of Eq. (11) and other factors. Specifically for the exponent a, geometrical considerations about the shape of the solid, are also important (Farin and Avnir, 1992; Valsami and Macheras, 1995).

The concentration of free solvent molecules can be written as

$$[w] = ([w_0] - \frac{1}{n}[c]) \tag{13}$$

where $[w_0]$ is the initial concentration of the free solvent species; the concentration of the undissolved drug species can be written as

$$[s] = \left(\frac{M_0}{V} - [c]\right). \tag{14}$$

where M_0 is the initial quantity, expressed in moles and V is the volume of the dissolution medium. Also, since $[c] << [w_0]$ we may assume that $[w] \approx [w]_0$, and therefore substituting in Eq. (12) we have:

$$\frac{d[c]}{dt} = k_1'\left(\frac{M_0}{V} - [c]\right)^a - k_{-1}[c] \quad (15)$$

where $k_1' = k_1[w_0]^b$. This simplification cannot be applied in other uses of this model, where the reactant species are not in excess. By one more step we can convert the concentration $[c]$ of the complex which is in moles per unit volume to concentration, C, of the dissolved quantity in mass per volume units by multiplying both sides of Eq. (15) with the molecular weight of the complex. Then, we end up with Eq. (16):

$$\frac{dC}{dt} = k_1^*\left(\frac{D}{V} - C\right)^a - k_{-1}C \quad (16)$$

Where $k_1^* = k_1'(\text{molecular weight})^{1-a}$ and D is the initial quantity (dose) in mass units.

Eq. (16) cannot be solved analytically in the general case, but it can be solved numerically and therefore can be fitted to dissolution data in order to estimate parameters, k_1^*, k_{-1} and a. Also, the exponent, a, can be estimated by the initial rate at $t = 0$:

$$\left.\frac{dC}{dt}\right|_{t=0} = k_1^*\left(\frac{D}{V}\right)^a \quad (17)$$

from an experiment that measures the initial rate as a function of different doses, D. Eqs. (16) and (17) reveal that the rate of dissolution is not dependent on drug solubility as it happens to be the case for diffusion limited dissolution.

Simpler, special cases of Eq. (16) can be considered, which may also have analytical solutions and in fact some of them produce classic results. Below, two special cases are mentioned, namely, (i) the homogenous case where $a = 1$ and (ii) the case where the solvent is in abundance (the dose is much lower than the amount needed to saturate the dissolution medium).

2.3. Homogeneous case

The case where $a = 1$ is the simplest, which also assumes that all the undissolved species have equal probability to dissolve, implying that they are in a form of a well-mixed dispersion. Eq. (16), by setting $a = 1$, becomes linear and dividing both parts by D/V we end up with

$$\frac{d\Phi}{dt} = k_1^*(1 - \Phi) - k_{-1}\Phi \quad (18)$$

Finally, after rearrangement we end up with:

$$\frac{d\Phi}{dt} = k_1^*(1 - q_{ss} \times \Phi) \quad (19)$$

where $q_{ss} = (k_1^* + k_{-1})/k_1^*$ is a dimensionless constant.

The solution of Eq. (19) is

$$\Phi = \frac{1}{q_{ss}}(1 - \exp(-q_{ss} \times k_1^* t)) = \frac{1}{q_{ss}}(1 - \exp(-(k_1^* + k_{-1})t)) \quad (20)$$

where Φ approaches asymptotically the value $1/q_{ss}$. We notice that the form of Eq. (20) is first-order, closely resembling the classic integrated form of Noyes–Whitney equation (Eq. (7)).

When $q_{ss} \approx 1$, sink conditions prevail and therefore Φ approaches unity, which means that the entire dose is dissolved. This is the case where $k_1^* \gg k_{-1}$ or $k_1^* + k_{-1} \approx k_1^*$ and corresponds to the unidirectional case of reaction, Eq. (11).

When $q_{ss} > 1$ the reaction reaches chemical equilibrium and Φ approaches the solubility level $1/q_{ss}$. In fact, when solubility is the steady state, that is when solubility $< D/V$, it can be calculated from the steady state condition of Eq. (18) by setting the left part equal to zero,

$$0 = k_1^*\left(\frac{D}{V} - C_{ss}\right)^a - k_{-1}C_{ss} \quad (21)$$

where C_{ss} is the steady state concentration. Eq. (21) cannot be generally solved for C_{ss}, however it could be solved numerically. Also, for the special case of $a = 1$ it yields:

$$C_{ss} = \frac{k_1^*}{k_1^* + k_{-1}} \times \frac{D}{V} = \frac{D}{q_{ss} \times V} \quad (22)$$

So, C_{ss} can be considered as the solubility and q_{ss} as the dimensionless dose–solubility ratio, $D/(C_{ss}V)$, but only when solubility is lower than D/V. Attention must be paid, because actually C_{ss} is the steady state and q_{ss} is the "dose-steady-state ratio" and correspond to solubility and dose-solubility ratio, respectively, only when the steady state is the solubility, that is when solubility is lower than D/V. Otherwise, when solubility is greater than D/V, the entire dose is dissolved, the backward reaction in Eq. (11) is negligible, $k_{-1} \approx 0$, the dimensionless dose–solubility ratio is less than 1, and the steady state is $C_{ss} = D/V$, since $q_{ss} = 1$.

2.4. Solvent in abundance (sink conditions)

As we already mentioned above the sink conditions in the homogeneous case of $a = 1$, correspond to $k_1^* \gg k_{-1}$. Similarly, when $a \neq 1$ in Eq. (15), one can define the case where the reaction, Eq. (11), becomes unidirectional, namely $k_{-1} \approx 0$. Consequently, Eq. (15) reduces to

$$\frac{dC}{dt} = k_1^*\left(\frac{D}{V} - C\right)^a \quad (23)$$

Eq. (23) has an analytical solution, which has the form of a power-law:

$$C = \frac{D}{V} - \left(\left(\frac{D}{V}\right)^{1-a} - (1-a)k_1^* t\right)^{1/(1-a)} \quad (24)$$

Power-laws have appeared before in literature for the mathematical description of release curves. (Siepmann and Peppas, 2001).

3. Experimental

In this study formulations of two relatively insoluble drugs were utilized, namely, naproxen and nitrofurantoin. Solubility

experiments in the various dissolution media utilized were carried out in order to get independent solubility estimates for comparative purposes. For the dissolution studies both the official paddle (naproxen) and the basket (nitrofurantoin) methods were utilized (USP, 2006).

3.1. Solubility studies

All solubility studies were performed at 37 °C, prior to dissolution experiments. For naproxen, solubility experiments were performed in phosphate buffer pH 7.4 and pH 6.8 and in acetate buffer pH 4.5. The solubility of nitrofurantoin was studied in acetate buffer pH 4.5 and in Simulated Gastric Fluid (SGF) (USP, 2006).

The experimental procedure was as follows: An excess of drug powder was added to a 25 ml flask containing 10 ml of the appropriate medium. The flasks were placed in a thermostated water bath at 37 °C under constant shaking rate of 100 rpm for 24 h.

The official HPLC-UV method described in USP 29 (2006) was applied for naproxen assay value (mobile phase: acetonitrile–water–glacial acetic acid at volume ratio of 50:49:1, flow rate 1.2 ml/min, column type: C-18 ODS 150 mm × 4.6 mm, 254 nm detector), while the concentration of nitrofurantoin was determined spectrophotometricaly at 375 nm.

Each experiment was run in triplicate.

3.2. Dissolution studies

Commercially available formulations of naproxen (Naprosyn®) and nitrofurantoin (Furolin®) were used in this study: More specifically, Naprosyn® IR tablets, 250 mg/tab (lot no. 0501027) and Furolin® IR tablets, 50 mg/tab (lot no. 40805) and 100 mg/tab (lot no. 050202) were used.

All dissolution tests were conducted in triplicate at 37 ± 0.5 °C.

Dissolution experiments were performed using various drug doses, volume and pH values of the dissolution medium, Table 1. For the data sets of Table 1 marked with *, N1 and F1 the respective Dose/V ratios were chosen in order to be close but lower than the saturation solubility values of the two drugs. As explained in Appendix B this condition allows the valid estimation of solubility using Eqs. (7), (9) and (10) from drug dissolution data reaching complete dissolution and assuming that the model(s) used is/are correct.

3.3. Naproxen tablets

Dissolution experiments (data sets N2, N3 and N4, Table 1) were performed according to USP 29 method, for Naprosyn® 250 mg/tab, using as dissolution medium 900 or 500 ml of phosphate buffer pH 7.4, or 500 ml phosphate buffer pH 6.8; the rotation speed was set at 50 rpm. The dissolution data set N1 of Table 1 was also studied using the USP 29 method. The preparation of 50 mg formulations (data set N1, Table 1) was performed as follows: Ten 250-mg tablets were accurately weighted and finely powdered. Three portions, equivalent to the mean tablet weight, were weighted, transferred to 100 ml volumetric flasks and diluted to volume with phosphate buffer pH 7.4. Solutions, after being filtered and properly diluted, were assayed by the official HPLC-UV method (USP, 2006). The determined naproxen concentration was used to calculate the mean content of naproxen in the tablets. Afterwards, a 250 mg tablet was cut appropriately, so as to get approximately the 1/5 of the tablet. This tablet fraction was intact, requiring disintegration on contact with the dissolution medium. The remaining 4/5 part of the tablet was finely powdered, transferred to a 100 ml volumetric flask and diluted to volume with phosphate buffer pH 7.4. The solution was filtered, properly diluted and assayed with the official HPLC-UV method (USP, 2006). The amount of naproxen in the remaining tablet was calculated from the determined naproxen concentration and subtracted from the estimated mean content of naproxen in the tablets. This corresponds to the amount of naproxen in the 1/5 portion of the tablet used in the study. This approach was followed for each one of the tablets used in the study.

The official HPLC-UV method described in USP 29 was applied for naproxen assay.

3.4. Nitrofurantoin tablets

Dissolution experiments using various strengths of nitrofurantoin (data sets F1–F4, Table 1) in 900 ml of dissolution medium were performed applying the method described in USP 29 (2006). More specifically, the following dissolution tests were carried out: (i) one Furolin® 100 mg tablet in 900 ml of acetate

Table 1
Datasets, formulations, dissolution conditions and experimental solubility values (C_s)

Dataset	Formulation	Amount (mg)	Volume (ml)	pH	C_s (mg/ml)
N1[a]	Naprosyn	50	900	4.5	0.0722 (0.011)
N2		250	500	7.4	22.12 (0.47)
N3		250	900	6.8	8.298 (0.19)
N4		250	500	6.8	8.298 (0.19)
F1[a]	Furolin	200	900	4.5	0.252 (0.03)
F2		100	900	4.5	0.252 (0.03)
F3		150	900	4.5	0.252 (0.03)
F4		100	900	1.2 SGF	0.2753 (0.013)

In parentheses the standard deviations of C_s.

[a] Formulations reaching complete dissolution, which fulfill the criteria derived in Appendix B for valid estimation of solubility using Eqs. (7), (9) and (10).

buffer pH 4.5 and 900 ml of SGF, (ii) one Furolin® 100 mg tablet and one Furolin® 50 mg tablet, in 900 ml of acetate buffer pH 4.5 and (iii) two Furolin® 100 mg tablets in 900 ml of acetate buffer pH 4.5.

4. Results

In the theoretical part above, an alternative approach to drug dissolution, based on the assumption that dissolution is a reaction-limited process was presented. The important difference between the present model and the diffusion layer model, is that while in the latter, the solubility is a thermodynamic parameter and drives the dissolution rate, here, the "solubility" term C_{ss} is the result of chemical equilibrium, (Eq. (22)), and is related non-linearly to the rate through the microconstants k_1^*, k_{-1} and the quantity D/V.

The profiles of the dissolved drug obtained from Eq. (16), have the anticipated shape of a monotonically raising, downwards concaving function that reaches a plateau. Plots of the numerical solution of Eq. (16) are shown in Fig. 1A for various values of the exponent a, in terms of fraction of dose dissolved, by dividing the concentration of drug in solution, C, by D/V. The profiles can mimic various cases of real life data including the abrupt approach to the plateau, when the entire dose is being dissolved (Fig. 1A, top curve).

An important consequence of the presence of the exponent a in Eq. (16), is that for $a \neq 1$, it becomes nonlinear. It is easy to see that in this case the rate is not independent of the dose as it happens to be the case for $a = 1$. This is shown in Fig. 1B, where for $a = 0.5$, three curves are plotted for different values of D/V. One can easily observe that the differences in the dose, produce different dissolution rates, i.e. the top curve being the fastest and the bottom one the slowest. A fact anticipated, since when both parts of Eq. (16) are divided by D/V, in order to express the dissolved drug as a fraction, dose is still present and does not vanish from the expression.

On the other hand when $a = 1$, Eq. (16) becomes first-order, i.e. Eq. (18) expressed in terms of fraction of dose dissolved, and its solution is an exponential approach to a plateau, Eq. (20). Then, the model is indistinguishable from the classic Noyes–Whitney model, which is based on different assumptions but results to the same first-order equation (Touitou and Donbrow, 1981; Kimura et al., 1994). However, as already mentioned, even the Noyes–Whitney equation is not always first order, since in the case where the entire dose can be dissolved, Noyes–Whitney law includes a discontinuity and is formulated as a branched equation, Eq. (7). So, first-order kinetics really applies only in the case where the dissolution rate is proportional to the available amount of drug, with each undissolved molecule having equal probability to dissolve. This model corresponds to the ideal homogeneous reaction-limited dissolution model and is described by Eq. (18). In (Lansky and Weiss, 2003) a measure of dissolution heterogeneity was introduced, which was defined as the departure or the distance from this ideal theoretical homogeneous case, although the authors did not attribute any physical meaning to this model.

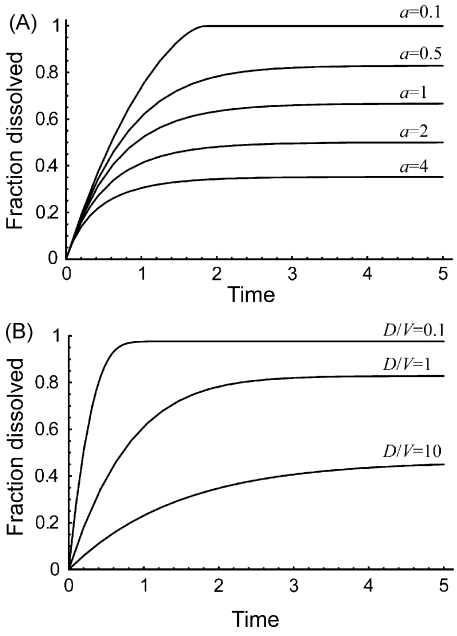

Fig. 1. Profiles of fraction of drug dose dissolved, using Eq. (16) and dividing C by D/V, are shown. Plot A shows profiles for various values of exponent a; the other parameters take values $k_1^* = 1$, $k_{-1} = 0.5$ and $D/V = 1$, all in arbitrary units. Plot B shows profiles for $a = 0.5$ and for various values of D/V; all other parameters take the same values as in (A).

We fitted Eq. (16) to dissolution data of naproxen and nitrofurantoin tablets, described in Section 3 and listed in Table 1. The reason why commercial formulations were chosen is that pure drugs cannot be properly studied in the official dissolu-

Table 2
Fitting results of Eq. (16) to the dissolution data of formulations listed in Table 1

Dataset	k_1^* (mg^{a-1} ml^{a-1} min^{-1})	k_{-1} (min^{-1})	a	R^2
N1	0.2726 (0.1348)	0.0001 (0.0001)	1.9969 (0.1492)	0.9911
N2	0.1464 (0.0099)	0 (0.0002)	1.1631 (0.0421)	0.9992
N3	0.1207 (0.0386)	0 (0.0009)	1.0834 (0.1524)	0.9866
N4	0.0799 (0.0132)	0 (0.0006)	1.0629 (0.118)	0.992
F1	0.558 (0.2205)	0 (0.0002)	2.3024 (0.19)	0.9894
F2	0.2504 (0.0486)	0 (0.0001)	1.5967 (0.0687)	0.9971
F3	0.4319 (0.1625)	0 (0.0006)	1.8112 (0.1638)	0.9914
F4	0.5079 (0.3218)	0.0002 (0.0003)	1.9501 (0.2304)	0.9768

In parentheses the standard errors of the estimates are shown.

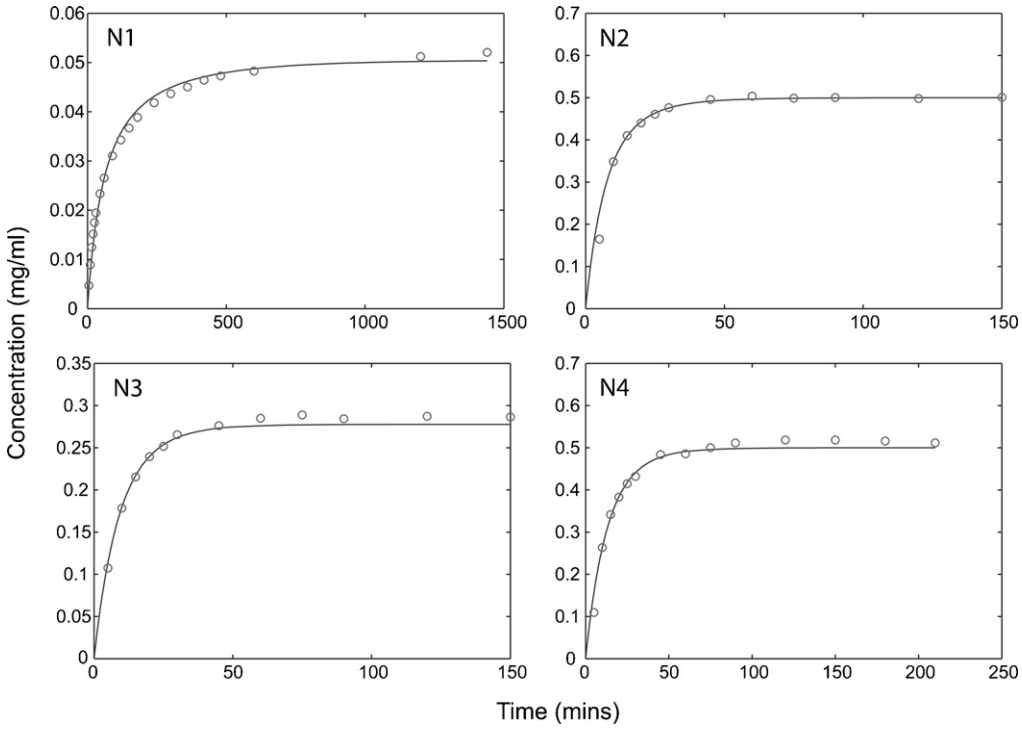

Fig. 2. Dissolution curves and fitted lines of Eq. (16) to all the experimental data points of the four naproxen (Naprosyn®) experiments of Table 1 (N1–N4).

tion test because of problems related to wetting and floating. Also, we are particularly interested to investigate the dissolution kinetics under the official dissolution tests conditions since this is correlated with the *in vivo* data. In Table 2 the estimated parameter values for k_1^*, k_{-1} and a, are presented together with their standard errors. Also, in Figs. 2 and 3 the fitted curves together with the experimental data are shown. Visual inspection of Figs. 2 and 3 together with the R^2 values reported in Table 2, reveal that the fittings are adequate. Fittings were performed using MATLAB's functions "lsqcurvefit" for the optimisation while the differential equation was solved numerically by using "ode45" MATLAB function.

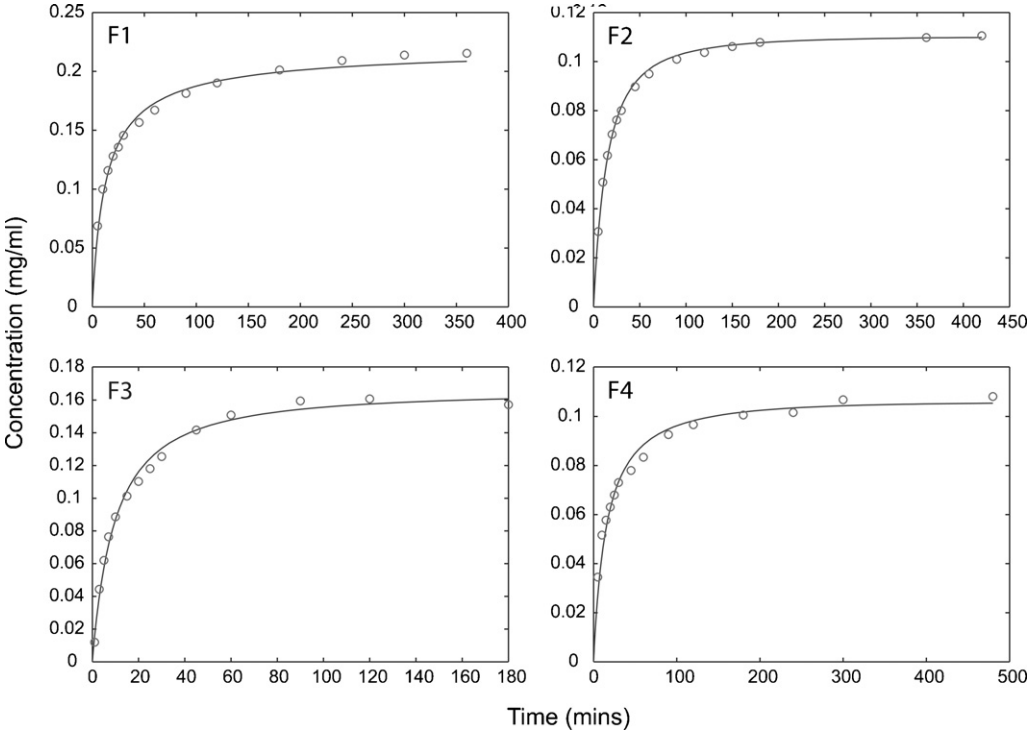

Fig. 3. Dissolution curves and fitted lines of Eq. (16) to all the experimental data points of the four nitrofurantoin (Furolin®) experiments of Table 1 (F1–F4).

Table 3
Fitting results of Eqs. (7), (9) and (10) to the dissolution data of formulations N1 and F1 listed in Table 1

Dataset	Eq. (7)					
	k_d (min^{-1})		q	$1/q$	Calc. $1/q$[a]	R^2
N1	0.0165 (0.0014)		1.2717 (0.0332)	0.7863	1.30	0.9691
F1	0.0718 (0.0089)		1.2753 (0.0474)	0.7841	1.13	0.9205
Dataset	Eq. (9)					
	k_s ($mg^{2/3}ml^{2/3}min^{-1}$)		q	$1/q$	Calc. $1/q$[a]	R^2
N1	0.1303 (0.0078)		1.2021 (0.0245)	0.8318	1.30	0.9904
F1	0.2362 (0.0213)		1.2136 (0.0356)	0.8239	1.13	0.9723
Dataset	Eq. (10)					
	γ ($min^{-\beta}$)	β	q	$1/q$	Calc. $1/q$[a]	R^2
N1	0.047 (0.0032)	0.6812 (0.0214)	1.1359 (0.021)	0.8803	1.30	0.9979
F1	0.1722 (0.0123)	0.5971 (0.0362)	1.128 (0.0318)	0.8865	1.13	0.9961

In parentheses the standard errors of the estimations are shown.
[a] Calculated $1/q$ values using Eq. (6) and the independent experimental solubility values listed in Table 1.

The solubility and dissolution data were also considered in the light of diffusion limited models, Eqs. (7), (9) and (10). The results of solubility experiments in all media utilized in the dissolution studies listed in Table 1 reveal that the data sets N1 and F1 can be used for the estimation of q using Eqs. (7), (9) and (10) (see Appendix B). Accordingly, we proceeded to the fitting of Eqs. (7), (9) and (10) to the datasets of Table 1 marked with *, N1 and F1, in order to estimate the values of q. These datasets were chosen because their real q values, as calculated from the experimental values of the solubility, are larger than 1, which means that they cannot be estimated directly from the plateau, but they are still inside the estimable region derived from the analysis using the Fisher Information Matrix (FIM, see Appendix A). The results are shown in Table 3, where, Eq. (9) and the first branch of Eqs. (7) and (10) were fitted to the data, using the data points corresponding up to the 85% of the fraction of the initial dose. This was done to avoid biasing the estimates of q from the values of the plateau. It should be noted that the amounts of drugs used, expressed in terms of concentration (Dose/V) are ~80% of the saturation solubility and therefore the proper estimation of q should be feasible in accord with the simulation studies (see Appendix B). In all cases reasonable fittings were observed, with square of correlation coefficient values ranging from 0.920 to 0.998. The estimates for q derived, with the corresponding standard error values and the respective $1/q$ values, are listed in Table 3. From the estimated values of $1/q$ one can see that these values are less than 1 and do not predict the calculated Eq. (6) values of $1/q$ (also listed in Table 3), by using the independent experimental solubility estimates listed in Table 1. The discrepancies between experimental and calculated $1/q$ values in Table 3 are not associated with the influence of tablets constituents on drug solubility since the experimental solubility values were verified in dissolution experiments (data not shown) with higher drug doses reaching saturation solubility with the same tablets in the same media. Also, deficiencies such as assumptions for mono-dispersed spherical particles and constant diffusion layer thickness not dependent on the particle size associated with the use of Eq. (8) do not seem to be important since similar results (Table 3) were obtained with Eq. (10) which takes into account all time-dependent changes. Overall, these results are evidence that under the conditions of the official dissolution test apparatuses, the saturation solubility is not justified to be considered as the driving force of the dissolution process and this is consistent with a range of reasonable models based on the diffusion limited dissolution assumptions. We have to point out that we are not trying to compare the goodness of fit between the different models. Due to the similarity in the shape of the output profiles of the different models (e.g. Eq. (16) collapses to the Noyes-Whiteny equation when $a = 1$) an exercise based on the goodness of fit would not reveal statistically significant differences. Instead we are assessing the validity of the underlying assumptions, and from our results the diffusion limited model assumption is not validated. On the other hand the proposed model, based on a reaction-limited assumption, presents itself

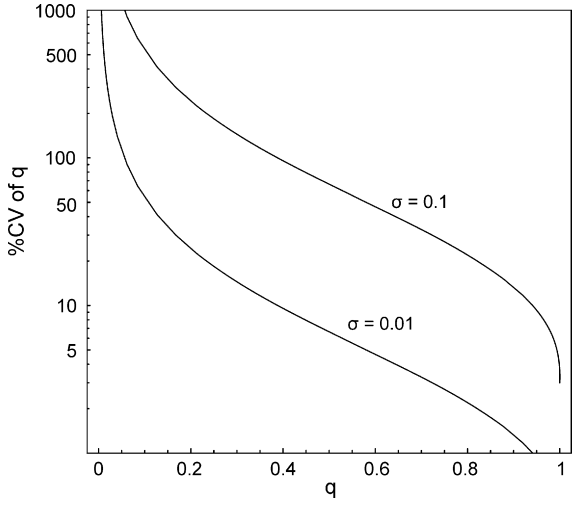

Fig. A.1. The uncertainty of q in %CV, for the model of Eq. (7) and for the range of q between 0 and 1, is plotted, for 2 different values of σ, namely, 0.01 and 0.1.

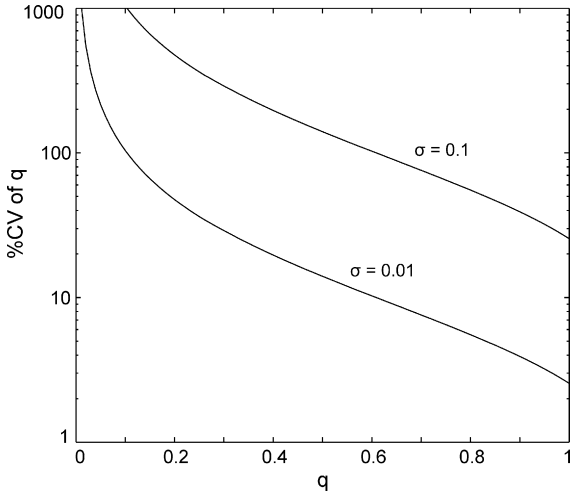

Fig. A.2. The uncertainty of q in %CV, for the model of Eq. (9), for $\beta = 1$ and for the range of q between 0 and 1 is plotted for two different values of σ, namely, 0.01 and 0.1.

as an attractive alternative with several advantages, especially under *in vivo* conditions.

5. Discussion

The theory of convective diffusion of a solute in liquids and its application to dissolution experiments has been based on the rotating disk apparatus where the surface area and the hydrodynamic conditions are perfectly controlled. However, recent studies based on computational fluid dynamics (McCarthy et al., 2003, 2004; D'Arcy et al., 2005, 2006) revealed not only the complexity of the fluid flow in the basket and paddle methods of dissolution, but also the chaotic aspects of hydrodynamics. Also, the molecular collision rate of the fluid with the solid particles in the official dissolution tests is well above the corresponding one in the rotating disk system because of the different positioning of the drug species in the medium (drug compact versus freely movable particles). In other words, the hydrodynamics is remarkably different among the dissolution systems mentioned. Since the hydrodynamics of the dissolution system is the key factor controlling the dissolution mechanism, it is unjustifiable to extrapolate the dominant role of diffusion, observed in rotating apparatuses, to the official dissolution systems.

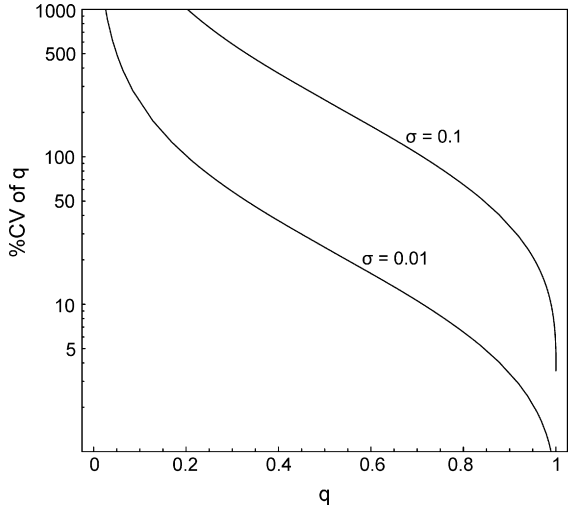

Fig. A.3. The uncertainty of q in %CV, for the model of Eq. (10) and for the range of q between 0 and 1 is plotted for two different values of σ, namely, 0.01 and 0.1.

Indeed, deviations from the diffusional principles and the prevalence of a reaction-limited dissolution mechanism in drug dissolution studies are not unknown even under the rotating disk conditions (Touitou and Donbrow, 1981; Nedich and Kildsig, 1972; Nicklasson et al., 1981, 1983). Also, discrepancies between the dependence of dissolution rate on solubility are not uncommon in literature. This is particular so in the area of surfactant-facilitated dissolution of drugs when different dissolution systems are utilized. All modelling approaches of surfactant-facilitated dissolution of water-insoluble drugs rely on diffusion layer model or its variants (Crison et al., 1996; Jinno et al., 2000). Usually, rotating disks experiments are carried out and reversible or irreversible reactions between the drug, the micelle and the drug–micelle complex are considered to take place in the diffusional boundary layer under the well-defined hydrodynamics of the rotating disk. Although interpretation of dissolution results with surfactants in rotating disk apparatus based on the diffusion layer model has been reported (Bakatselou et al., 1991; Naylor et al., 1995), parallel powder dissolution experiments in the USP paddle apparatus cannot be explained using diffusion-convection principles and different mechanisms in the two types of devices have been proposed.

Departures from the diffusion layer model rationale have been repeatedly reported in gastrointestinal absorption studies (Persson et al., 2005). In these cases the dissolution rate does not seem to be proportional to the difference between the concentration of dissolved drug and the saturation solubility, as suggested by the diffusion layer model. The presence of reaction-limited drug dissolution in the gastrointestinal tract may explain this discrepancy. Moreover, a considerable variability of the absorption results in this type of studies may be associated with the four parameters involved in Eq. (16), namely, k_1^*, k_{-1}, a and their dependence on the variable and heterogeneous conditions and volume content of the gastrointestinal tract (Macheras and Argyrakis, 1997; Weitschies et al., 2005).

Finally, the prevailing role of solubility as the key parameter for biopharmaceutic classification of drugs (FDA, 2000) has been based on the assumption that both *in vitro* and *in vivo* drug dissolution follows diffusional principles. The results of the present study indicate that the reaction between the undissolved species and the dissolution medium molecules drives the dissolution process in the official dissolution systems. Therefore, a model independent parameter e.g. mean dissolution time, seems to be more appropriate for classification purposes because of the uncertainty regarding the dissolution mechanism(s) under *in vitro* and/or *in vivo* conditions.

6. Conclusion

Deviations from the diffusional principles is not uncommon in dissolution literature and this study provides a clear evidence

that the dissolution rate of formulations of the two model drugs in the official dissolution systems does not follow the diffusion layer model.

A reaction-limited dissolution model is presented, where dissolution is considered to be a reaction between the undissolved species and the dissolution medium molecules. The rate of dissolution is therefore driven by the concentration of the undissolved species and solubility is considered to be the concentration when the reaction equilibrium is reached. The model exhibits rich behavior mimicking the profiles obtained by the classic equations but also shows additional flexibility, which may prove useful in dissolution curve fitting. The assumptions utilised by the model may be particularly applicable to *in vivo* conditions, potentially explaining the observed variability and deviations from the diffusion layer model principles. The approach could also be applicable for surfactant facilitated dissolution of drugs. Overall, the present model provides an interesting alternative to the classic approaches of drug dissolution modeling, quantifying the case of reaction-limited dissolution of drugs, a scenario that has not been discarded on physical grounds, but has not been very popular in actual practice either, partly because of the lack of a simple model for it.

Appendix A

A.1. Estimability of the saturation solubility from dissolution data reaching complete dissolution using Eqs. (7), (9) and (10)

The uncertainty associated with parameters q or q_i that arises when they are estimated from dissolution data reaching complete dissolution using Eqs. (7), (9) and (10) was explored using the Fisher Information Matrix (FIM) (Atkinson and Donev, 1992). The reason why we study the FIM comes from the Cramer-Rao inequality which states that the inverse of the FIM is a lower bound to the variance-covariance matrix of any unbiased estimator of the model parameters.

To this end, the FIM was calculated for a typical experimental design of a dissolution test with 5 data points at $0.16T$, $0.32T$, $0.48T$, $0.64T$, $0.80T$; the time parameter T is described by Eqs. (A.1) and (A.2) for Eqs. (7) and (10), respectively and corresponds to the time for the completion of the dissolution process (Dokoumetzidis et al., 2006) ($\Phi = 1$):

$$T = -\frac{\ln(1-q)}{k_d} \tag{A.1}$$

and

$$T = \left(-\frac{\ln(1-q)}{\gamma}\right)^{1/\beta} \tag{A.2}$$

For Eq. (9) since the time when dissolution finishes is infinite, T was chosen to be the time when the 90% of the initial amount has been dissolved, $T_{90\%}$. The points chosen in this case were $0.16T_{90\%}$, $0.32T_{90\%}$, $0.48T_{90\%}$, $0.64T_{90\%}$, $0.80T_{90\%}$.

The FIM, M, takes the form:

$$M = \frac{N}{\sigma^2}\sum_{j=1}^{n}\left(\frac{\partial\Phi(\theta,t_j)}{\partial\theta}\right)\left(\frac{\partial\Phi(\theta,t_j)}{\partial\theta}\right)' \tag{A.3}$$

where, θ is a vector of the model parameters (q, k_d) for the model of Eq. (7) and (q, γ, β) for the model of Eq. (10) and therefore the terms $\partial\Phi(\theta, t_j)/\partial\theta$ are vectors too containing the partial derivatives for each model parameter. The prime stands for the transpose matrix, σ^2 is the variance of the residual error which is assumed to be additive and normally distributed and N is the number of replicate experiments.

The FIM, M, for the model of Eq. (5) is calculated from Eq. (A.3) and reads:

$$M = \frac{N}{\sigma^2}\sum_{j=1}^{n}\begin{pmatrix}\left(\frac{\partial\Phi(q,k_d,t_j)}{\partial q}\right)^2 & \frac{\partial\Phi(q,k_d,t_j)}{\partial q}\frac{\partial\Phi(q,k_d,t_j)}{\partial k_d}\\ \frac{\partial\Phi(q,k_d,t_j)}{\partial q}\frac{\partial\Phi(q,k_d,t_j)}{\partial k_d} & \left(\frac{\partial\Phi(q,k_d,t_j)}{\partial k_d}\right)^2\end{pmatrix}$$

By replacing Eq. (5) it becomes:

$$M = \frac{N}{\sigma^2}\sum_{j=1}^{n}\begin{pmatrix}\frac{(1-e^{-k_d t_j})^2}{q^4} & \frac{e^{-kt_j}(1-e^{-k_d t_j})t_j}{q^3}\\ \frac{e^{-k_d t_j}(1-e^{-k_d t_j})t_j}{q^3} & \frac{e^{-2k_d t_j}t_j^2}{q^2}\end{pmatrix}$$

Which is the final form of the FIM used in the analysis. The FIM for the Weibull function was obtained in a similar manner.

Similar relationships to Eqs. (A.1)–(A.3) can be written for Eqs. (7) and (10) by replacing q with q_i. Then, the standard error of the estimate for q as a percentage coefficient of variation, CV is given by

$$\%\mathrm{CV} = \frac{100}{q}\sqrt{(M^{-1})_{1,1}} \tag{A.4}$$

where $(M^{-1})_{1,1}$ is the 1st column, 1st row element of the inverse matrix. Note that for the model of Eq. (7), by choosing a design where the points take values which are fractions of T, we are able to eliminate k_d, as Eq. (11) can be solved for k_d and then replaced in the FIM making $(M^{-1})_{1,1}$ to depend only on q. This set of experimental points is as good as any other but more convenient to use in our analysis. The uncertainty of k_d is still taken into account in the analysis, so k_d is not considered known or fixed. Similarly, for the model of Eq. (10), γ is eliminated, although β still remains. However, for the model of Eq. (9) an analytical solution is not available and the whole procedure of estimating the FIM was done numerically, using the numerical solution of the differential equation.

Appendix B

B.1. Estimation of saturation solubility from dissolution data reaching complete dissolution using Eqs. (7), (9) and (10): simulation studies

Eqs. (7), (9) or (10) may be fitted to dissolution data in order to estimate the parameter q, and then a value for the uncertainty of q can be also obtained. From Eq. (A.4) the uncertainty, in %CV units, of the estimation of q, in respect to a specific value of q and for a given value of the residual error σ can be estimated. In Fig. A.1, the uncertainty of q for the model of Eq. (7) and for the entire range of $q<1$ values, from 0 to 1, is plotted, for two different values of σ, namely 0.01, and 0.1. The number of replicate experiments has been considered to be $N=1$. One can see from the plots of Fig. A.1 that relatively low uncertainty for the estimation of q arises only when q has a relatively high value, close to 1, which corresponds to solubility values, C_s, being relatively close to the concentrations corresponding to the dose, Dose/V. For example, for a value for $\sigma=0.1$, reasonable estimates for q, i.e. values of %CV below 50%, may be obtained only for values of q greater than 0.6. This corresponds to a solubility value, C_s, being only 66% higher from the concentration value, Dose/V that corresponds to the dose. Similarly with Fig. A.1, in Figs. A.2 and A.3, for the models of Eqs. (9) and (10), respectively, the %CV of the uncertainty of q is plotted against the actual value of q while in Fig. A.3 $\beta=1$. The curves have a similar form but for the same value of q, the corresponding uncertainty is higher. Note that although for $\beta=1$ the model of Eq. (10) collapses to Eq. (7), the parameter β is still considered to be estimated and uncertainty is associated with it, hence it contributes to the uncertainty of parameter q, as there is correlation between all model parameters. So, the conclusion from the analysis with the FIM, is that in principle, parameter q may be estimated from dissolution data, even when $q<1$, although, the further q is away from 1, the larger is the uncertainty associated with this estimation.

References

Atkinson, A.C., Donev, A.N., 1992. Optimum Experimental Designs. Clarendon Press, Oxford.

Bakatselou, V., Oppenheim, R.C., Dressman, J.B., 1991. Solubilization and wetting effects of bile salts on the dissolution of steroids. Pharm. Res. 8, 1461–1469.

Brunner, E., 1904. Reaktionsgeschwindigkeit in heterogenen Systemen. Z. Phys. Chem. 43, 56–102.

Crison, J.R., Shah, V.P., Skelly, J.P., Amidon, G.L., 1996. Drug dissolution into micellar solutions: development of a convective diffusion model and comparison to the film equilibrium model with application to surfactant-facilitated dissolution of carbamazepine. J. Pharm. Sci. 85, 1005–1011.

D'Arcy, D.M., Corrigan, O.I., Healy, A.M., 2005. Hydrodynamic simulation (CFD) of asymmetrically positioned tablets in the paddle dissolution apparatus: impact on dissolution rate and variability. J. Pharm. Pharmacol. 57, 1243–1250.

Daccord, G., 1989. Dissolutions, evaporations, etchings. In: Avnir, D. (Ed.), The Fractal Approach to Heterogeneous Chemistry. John Willey & Sons, Chichester, pp. 183–197.

D'Arcy, D.M., Corrigan, O.I., Healy, A.M., 2006. Evaluation of hydrodynamics in the basket dissolution apparatus using computational fluid dynamics–dissolution rate implications. Eur. J. Pharm. Sci. 27, 259–267.

Dejmek, M., Ward, C.A., 1998. A statistical rate theory study of interface concentration during crystal growth or dissolution. J. Chem. Phys. 108, 8698–8704.

Dokoumetzidis, A., Macheras, P., 1997. A population growth model of dissolution. Pharm. Res. 14, 1122–1126.

Dokoumetzidis, A., Macheras, P., 2006. A century of dissolution research: from Noyes and Whitney to the biopharmaceutics classification system. Int. J. Pharmaceut. 321, 1–11.

Dokoumetzidis, A., Papadopoulou, V., Macheras, P., 2006. Analysis of dissolution data using modified versions of Noyes–Whitney equation and the Weibull function. Pharm. Res. 23, 256–261.

Farin, D., Avnir, D., 1992. Use of fractal geometry to determine effects of surface morphology on drug dissolution. J. Pharm. Sci. 81, 54–57.

FDA, 2000. Guidance for Industry, Waiver of in vivo bioavailability and bioequivalence studies for immediate release solid oral dosage forms based on a biopharmaceutics classification system. FDA/CDER, Washington D.C.

Greenberg, J., Tomson, M., 1992. Precipitation and dissolution kinetics and equilibria of aqueous ferrous carbonate vs. temperature. Appl. Geochem. 7, 185–190.

Higuchi, W.I., 1967. Diffusional models useful in biopharmaceutics. J. Pharm. Sci. 56, 315–324.

Ji, X., Chen, D., Wei, T., Lu, X., Wang, Y., Shi, J., 2001. Determination of dissolution kinetics of K_2SO_4 crystal with ion selective electrode. Chem. Eng. Sci. 56, 7017–7024.

Jinno, J., Oh, D., Crison, J.R., Amidon, G.L., 2000. Dissolution of ionizable water-insoluble drugs: the combined effect of pH and surfactant. J. Pharm. Sci. 89, 268–274.

Khoury, N., Mauger, J.W., Howard, S., 1988. Dissolution rate studies from a stationary disk/rotating fluid system. Pharm. Res. 5, 495–500.

Kimura, M., Djilali, N., Dost, S., 1994. Convective transport and interface kinetics in liquid phase epitaxy. J. Cryst. Growth. 143, 334–348.

Lansky, P., Weiss, M., 1999. Does the dose-solubility ratio affect the mean dissolution time of drugs? Pharm. Res. 16, 1470–1476.

Lansky, P., Weiss, M., 2003. Classification of dissolution profiles in terms of fractional dissolution rate and a novel measure of heterogeneity. J. Pharm. Sci. 92, 1632–1647.

Levich, V., 1962. Physicochemical Hydrodynamics. Prentice Hall, Englewood Cliffs, NJ.

Lin, H., Rosenberger, F., Alexander, J.I.D., Nadarajah, A., 1995. Convective-diffusive transport in protein crystal growth. J. Cryst. Growth 151, 153–162.

Macheras, P., Argyrakis, P., 1997. Gastrointestinal drug absorption: is it time to consider heterogeneity as well as homogeneity? Pharm. Res. 14, 842–847.

Macheras, P., Dokoumetzidis, A., 2000. On the heterogeneity of drug dissolution and release. Pharm. Res. 17, 108–112.

Macheras, P., Iliadis, A., 2006. Modeling in Biopharmaceutics, Pharmacokinetics and Pharmacodynamics: Homogeneous and Heterogeneous Approaches. Springer, New York.

McCarthy, L.G., Bradley, G., Sexton, J.C., Corrigan, O.I., Healy, A.M., 2004. Computational fluid dynamics modelling of the paddle dissolution apparatus: agitation rate, mixing patterns and fluid velocities. AAPS PharmSciTech., 5, Article 31.

McCarthy, L.G., Kosiol, C., Healy, A.M., Bradley, G., Sexton, J.C., Corrigan, O.I., 2003. Simulating the hydrodynamic conditions in the United States Pharmacopeia paddle dissolution apparatus. AAPS PharmSciTech., 4, Article 22.

Miller-Chou, B.A., Koenig, J.L., 2003. A review of polymer dissolution. Prog. Polym. Sci. 28, 1223–1270.

Missel, P.J., Stevens, L.E., Mauger, J.W., 2004a. Dissolution of anecortave acetate in a cylindrical flow cell: Re-evaluation of convective diffusion/drug dissolution for sparingly soluble drugs. Pharm. Drug Dev. Technol. 9, 453–459.

Missel, P.J., Stevens, L.E., Mauger, J.W., 2004b. Re-examination of convective diffusion/drug dissolution in a laminar flow channel: accurate prediction of dissolution rate. Pharm. Res. 12, 2300–2306.

Naylor, L.J., Bakatselou, V., Rodriguez-Hornedo, N., Weiner, N.D., Dressman, J.B., 1995. Dissolution of steroids in bile salt solutions is modified by the presence of lecithin. Eur. J. Pharm. Biopharm. 41, 346–353.

Nedich, R.L., Kildsig, D.O., 1972. Mechanism of dissolution. I. Mathematical interpretation of concentration gradients developed during dissolution of a solid. J. Pharm. Sci. 61, 214–218.

Nernst, W., 1904. Theorie der Reaktionsgeschwindigkeit in heterogenen Systemen. Z. Phys. Chem. 47, 52–55.

Nicklasson, M., Brodin, A., Nyqvist, H., 1981. Studies on the relationship between solubility and intrinsic rate of dissolution as a function of pH. Acta Pharm. Suec. 18, 119–128.

Nicklasson, M., Brodin, A., Sundelöf, L.O., 1983. On the determination of true dissolution rate parameters from rotating disc experiments. Int. J. Pharm. 15, 87–95.

Noyes, A.A., Whitney, W.R., 1897. The rate of solution of solid substances in their own solutions. J. Am. Chem. Soc. 19, 930–934.

Persson, E.M., Gustafsson, A.S., Carlsson, A.S., Nilsson, R.G., Knutson, L., Forsell, P., Hanisch, G., Lennernas, H., Abrahamsson, B., 2005. The effects of food on the dissolution of poorly soluble drugs in human and in model small intestinal fluids. Pharm. Res. 22, 2141–2151.

Robertson, E.A., Fogler, H.S., 1996. Model for the reaction-rate-limited dissolution of solids with etch-rate heterogeneities. AICHE J. 42, 2654–2660.

Siepmann, J., Peppas, N.A., 2001. Modeling of drug release from delivery systems based on hydroxypropyl methylcellulose (HPMC). Adv. Drug. Deliv. Rev. 48, 139–157.

Sunagawa, I., Tsukamoto, K., Maiwa, K., Onuma, K., 1995. Growth and perfection of crystals from aqueous solution: case studies on barium nitrate and Kalum. Prog. Cryst. Growth Charact. Mater. 30, 153–190.

Swarbrick, J., 1970. In vitro models of drug dissolution. In: Swarbrick, J. (Ed.), Current Concepts in the Pharmaceutical Sciences: Biopharmaceutics. Lea & Febiger, Philadelphia, pp. 265–296.

Tao, J.C., Cussler, E.L., Evans, D.F., 1974. Accelerating gallstone dissolution. Proc. Nat. Acad. Sci. 71, 3917–3921.

Touitou, E., Donbrow, M., 1981. Deviation of dissolution behavior of benzoic-acid from theoretical predictions with lowering of temperature-Limitations as a model dissolution substance. Int J. Pharmaceut. 9, 97–106.

USP, 2006, USP 29 - NF 24. Official Monographs for Naproxen, Nitrofurantoin.

Valsami, G., Macheras, P., 1995. Determination of fractal reaction dimension in dissolution studies. Eur. J. Pharm. Sci. 3, 163–169.

Wagner, J., 1961. Biopharmaceutics: absorption aspects. J. Pharm. Sci. 50, 359–386.

Weitschies, W., Kosch, O., Monnikes, H., Trahms, L., 2005. Magnetic marker monitoring: An application of biomagnetic measurement instrumentation and principles for the determination of the gastrointestinal behavior of magnetically marked solid dosage forms. Adv. Drug. Deliv. Rev. 57, 1210–1222.

Wurster, D.E., Taylor, P.W., 1965. Dissolution rates. J. Pharm. Sci. 54, 169–175.

Yang, C.F., Cussler, E.L., 2001. Oxygen barriers that use free radical chemistry. AICHE J. 47, 2725–2732.